Testing Gravity on Cosmological Scales

Author: Tien Bui
Supervisors: Agnès Ferté, Vasiliy Demchenko

Institute for Astronomy
University of Edinburgh

September 28, 2016

Acknowledgements

This project was funded through the Career Development Internship Programme grant of the School of Physics and Astronomy, University of Edinburgh, UK.

Summary

Einstein's General Theory of Relativity (GR) is currently the most successful theory we have for describing the behaviour of gravity, the attractive force that keeps all masses together. According to this theory, the universe we live in should be undergoing a slowing-down expansion, but instead, from observations, we found its expansion to be speeding up. Several solutions have been proposed. They can be classified into two groups: one proposes the existence of a new, mysterious kind of energy (dark energy) that pushes matter apart; the other one suggests a change in our current laws of gravity. In this project, we assessed the second possibility of modifying GR to explain the accelerated expansion of the universe. We studied two models that are representative of two popular approaches in this direction: the $f(R)$ theories which are theoretical and the Bean-Tangmatitham parametrization which is phenomenological. These theories have parameters that can be modified to generate different behaviours of gravity, including those described by GR. We used the *emcee* algorithm and data from the Cosmic Microwave Background (CMB) anisotropy measurements and the weak lensing surveys to estimate the parameters of these modified gravity (MG) models. Estimations for the parameters were obtained at 95% confidence level. Estimations for the cosmological parameters are close but not consistent with those stated by the Planck collaboration [1]. The problem was found to be in the settings of our programme which caused a shift in the results. Meanwhile, estimations for the MG parameters suggest no deviation from GR. We did not have enough time at the end but it might also be useful to estimate the parameters with different algorithms and compare the results.

Personal Statement

The summer project has given me an invaluable experience. I have gained knowledge in cosmology, an area that is quite new to me, and besides, I have also learned many useful IT skills such as writing computer codes on Python, or using LaTeX to write documents, as well as the skills of gathering information from different sources. These are skills that are definitely valuable for people working in any area, especially researchers. I was lucky enough to be working with very nice and enthusiastic supervisors, who were always informative and willing to help. They guided me and helped me become acquainted with doing research on an area that I had little knowledge about. After the project, I feel more confident in myself. I would like to thank the School of Physics and Astronomy, University of Edinburgh for giving me this amazing opportunity of working in the academia. I will definitely go on to higher study and do more interesting researches like this in the future.

1 Introduction

Our understanding of the universe has rapidly improved with theoretical developments and advancements of cosmological observations. High precision cosmological probes suggest that our universe started as an extremely hot and dense region about 13.8 billion years ago [1] and has been expanding, growing to the size we see today. According to our understanding of gravity - the attractive force that keeps all masses together, whose behaviour is described by Einstein's General Theory of Relativity (GR) - the expansion should be decelerating, however, recent evidence suggests an accelerated expansion [2]. Many approaches have been pursued in attempt to explain the origin of this acceleration, but there are two that are most popular: one proposes that the universe consists of a dark energy field which opposes gravitational attraction; the other one suggests a modification to GR on large scale. This project explores the second approach. We assess a few representative Modified Gravity (MG) models and constrain their parameters using CosmoSIS - a cosmological parameter estimation code developed by J. Zuntz *et al.* [3].

This report is divided into six parts. Part 1 presents the motivation for our project. In Part 2, we describe in detail the MG models that were assessed. Part 3 introduces the cosmological probes used to constrain MG parameters. Part 4 describes the algorithms our methodology to get the constraints. In Part 5, we present, compare and constrast the constraints obtained using different data sets for each MG model. Finally, in Part 6, we conclude and discuss our results, proposing possible improvements for better constraints.

2 Modified Gravity Models

Currently, there are two main approaches to MG: either by modifying the action of GR, or by modifying directly the gravitational potentials perturbing the Friedmann-Lemaitre-Robertson-Walker metric:

$$ds^2 = a(t)^2[-(1+2\Psi)d\tau^2 + (1-2\Phi)dx^2] \tag{1}$$

where $\tau = t/a$ is the conformal time; $a(t)$ is the scale factor; $\Phi(a,k)$ and $\Psi(a,k)$ are the two gravitational potentials. These functions fully describe the metric. The potentials, $\Phi(a,k)$ and $\Psi(a,k)$, are determined by the Poisson and the perturbed Einstein equations [4]

$$k^2\Phi = -4\pi G a^2 \sum_i \rho_i \Delta_i \tag{2}$$

$$\Psi - \Phi = -12\pi G a^2 \sum_i \rho_i (1+w_i)\frac{\sigma_i}{k^2} \tag{3}$$

where k is the comoving wavenumber, ρ_i is the density of matter species i, $w_i = P/\rho$ is the matter's equation of state, σ_i is the anisotropic shear stress, $\Delta_i \equiv \delta_i + 3H(1+w)\theta_i/k^2$ is the rest-frame density perturbation with $H(a) = \dot{a}/a$ being the Hubble expansion factor, $\delta(k,a) \equiv \rho(k,a)/\bar{\rho}(a) - 1$ being the fractional over-density distribution, and θ being the divergence of the peculiar velocity.
By modifying these equations, we can alter the form of $\Phi(a,k)$ and $\Psi(a,k)$ and thus the metric.

2.1 f(R) theories

$f(R)$ theories introduce a function of the Ricci scalar, R, into the Einstein-Hilbert action [5] to generalize it as:

$$S[g] = \int \frac{1}{2\kappa} f(R)\sqrt{-g}\ \mathrm{d}^4x \tag{4}$$

where $g = \det(g_{\mu\nu})$ is the determinant of the metric tensor matrix, and $\kappa = 8\pi G c^{-4}$ is Einstein's constant, with G being the gravitational constant and c being the speed of light in vacuum.
The simplest case is $f(R) = R$ itself, which corresponds to GR.

Modifications to the Poisson and the perturbed Einstein equations are encoded in the two functions $\mu(a, k)$ and $\gamma(a, k)$ which are defined such that [6]

$$k^2\Psi = -\frac{a^2}{2M_p^2}\mu(a,k)\rho\Delta \tag{5}$$

$$\frac{\Phi}{\Psi} \equiv \gamma(a,k) \tag{6}$$

where $\rho\Delta$ is the comoving density perturbation and is defined as

$$\rho\Delta \equiv \rho\delta + 3\frac{aH}{k}(\rho + P)v \tag{7}$$

with P being pressure.

In f(R) theories, $\mu(a, k)$ and $\gamma(a, k)$ can be parametrized in the following way, as discussed in [7]

$$\mu(a,k) = \frac{1 + \beta_1\lambda_1^2k^2a^s}{1 + \lambda_1^2k^2a^s} \tag{8}$$

$$\gamma(a,k) = \frac{1 + \beta_2\lambda_2^2k^2a^s}{1 + \lambda_2^2k^2a^s} \tag{9}$$

where β_i are the dimensionless couplings, λ_i are dimensionful lengthscales, s is determined by the time evolution of the characteristic lengthscale of the theory and is constrained to take a value between 1 and 4. β_i and λ_i are related by

$$\beta_1 = \frac{\lambda_2^2}{\lambda_1^2} = 2 - \beta_2\frac{\lambda_2^2}{\lambda_1^2} \tag{10}$$

Moreover, we have the coupling constant $\alpha_i = \sqrt{2/3}\ \phi$, hence $\beta_1 = 4/3$ [8], and $s = 4$ as we want our model to closely mimic the Standard Model of Cosmology (the so-called ΛCDM model). Therefore, we only have one free parameter for equations 8 and 9, which is the lengthscale λ_1. It can be further parametrized in terms of B_0

$$\lambda_1^2 = B_0c^2/(2H_0^2) \tag{11}$$

where H_0 is the Hubble's constant. $B_0 = 0$ corresponds to GR.

2.2 Bean-Tangmatitham parametrization

Unlike f(R) theories, which originate from a proper theoretical background, the Bean-Tangmatitham (BT) parametrization is rather a phenomenological modification to the standard growth history of anisotropies.

In GR, the growth of structure in the universe is completely described by a set of 4 equations [9]

$$\dot{\delta} = -(1+w)(\theta - 3\dot{\phi}) - 3H(c_s^2 - w)\delta \tag{12}$$

$$\frac{\dot{\theta}}{k^2} = -H(1+3w)\frac{\theta}{k^2} - \frac{\dot{w}}{(1+w)}\frac{\theta}{k^2} + \frac{c_s^2}{1+w}\delta - \sigma + \psi \tag{13}$$

together with Poisson equations 2 and 3, where $c_S^2 = \partial P/\partial\rho$ is the sound speed; $H(a) = \dot{a}(t)/a(t)$ is the Hubble's expansion factor.
The BT parametrization modifies equations 2 and 3 with the two scale and time dependent fuctions $Q(k,a)$ and $R(k,a)$, while equations 12 and 13 are kept unchanged, assuming matter remains minimally coupled to gravity [4]. So equations 2 and 3 can be re-written as

$$k^2\phi = -4\pi G Q a^2 \sum_i \rho_i \Delta_i \tag{14}$$

$$\psi - R\phi = -12\pi G Q a^2 \sum_i \rho_i (1+w)\frac{\sigma_i}{k^2} \tag{15}$$

We will concentrate on late times, when the anisotropic stress, σ_i, is small, and we have

$$Q = \mu\gamma \tag{16}$$

$$R = \gamma^- 1 \tag{17}$$

with γ and μ are as defined in Section 2.1.
The growth history thus depends on the form of $Q(k,a)$ and $R(k,a)$. There are two possibilities:

- Q and R are fixed
- Q and R evolve with scale and time.

If the latter is the case, Q and R can be written as [4]

$$Q(k,a) - 1 = [Q_0 e^{-k/k_c} + Q_\infty(1 - e^{-k/k_c}) - 1]a^s \tag{18}$$

$$R(k,a) - 1 = [R_0 e^{-k/k_c} + R_\infty(1 - e^{-k/k_c}) - 1]a^s \tag{19}$$

where Q_0, R_0, Q_∞ and R_∞ are the asymptotic values of the modifications on super-horizon and sub-horizon scales today. The latter two are redundant because k_c is set to ∞. With that in mind, we have three free parameters, which are Q_0, R_0 and s. Q must be greater than 0, indicating that matter is attracted to over-densities, $R > -1$ because null geodesic paths are bent inwards by gravitational potentials, s has a lower limit of 0 which corresponds to a time-independent evolution [4]. $Q = 1.0$ and $R = 1.0$ correspond to GR in both cases.

3 Cosmological Probes

We used the Cosmic Microwave Background (CMB) anisotropy measurements from the Planck experiment [10] and the weak lensing data from the Canada-France-Hawaii Telescope Lensing Survey (CFHTLenS) [11] to constrain our MG models. This section describes the properties of these data and how they are useful for our purpose.

3.1 Cosmic microwave background

The CMB is the thermal radiation that is left over from the time of recombination in the universe history, when the universe had cooled down enough for atoms to be formed. This radiation is strongest in the microwave region of the light spectrum. Figure 1 shows an all-sky map of the CMB as obtained in the Planck experiment [10].

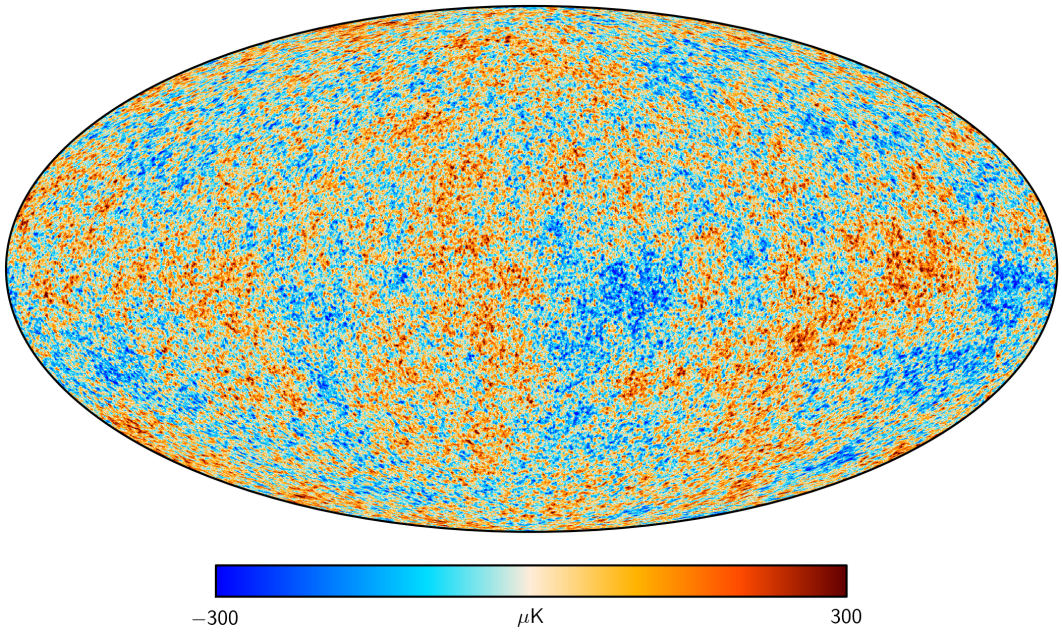

Figure 1: All-sky map of the CMB temperature as obtained by Planck.

The CMB is almost isotropic, but sensitive enough measurements had revealed small but detectable temperature and polarisation anisotropies in the CMB. These anisotropies play a crucial role in the evolution history and the properties of the universe. Some of the temperature anisotropies arise due to the integrated Sachs-Wolfe effect [12]: when the CMB radiation travels through gravitational potential wells or hills (regions of over-densities or voids), it gains or loses some of its energy; if these regions were static, the radiation would get back its initial energy after passing them. But because of the accelated expansion of the universe, these gravitational potential wells/hills evolve with time and thus cause a change in

the energy of the CMB radiation. Modifying gravitational laws will change the properties of the potential wells and therefore will also change the properties of the anisotropies. Effects of MG on the temperature power spectrum is shown in figure 2 [13, 14, 15, 16, 17, 7]. The power spectrum is related to the correlation of the temperature between two points in the sky and it characterizes the size of the temperature fluctuations. In figure 2, the temperature power spectrum is plotted as a function of the multipole moment, l, which is approximately inversely proportional to the angular scale. The spectrum predicted by MG models deviates from GR most noticeably at low multipoles, corresponding to large angular scales, whereas at high multipoles, they agree well.

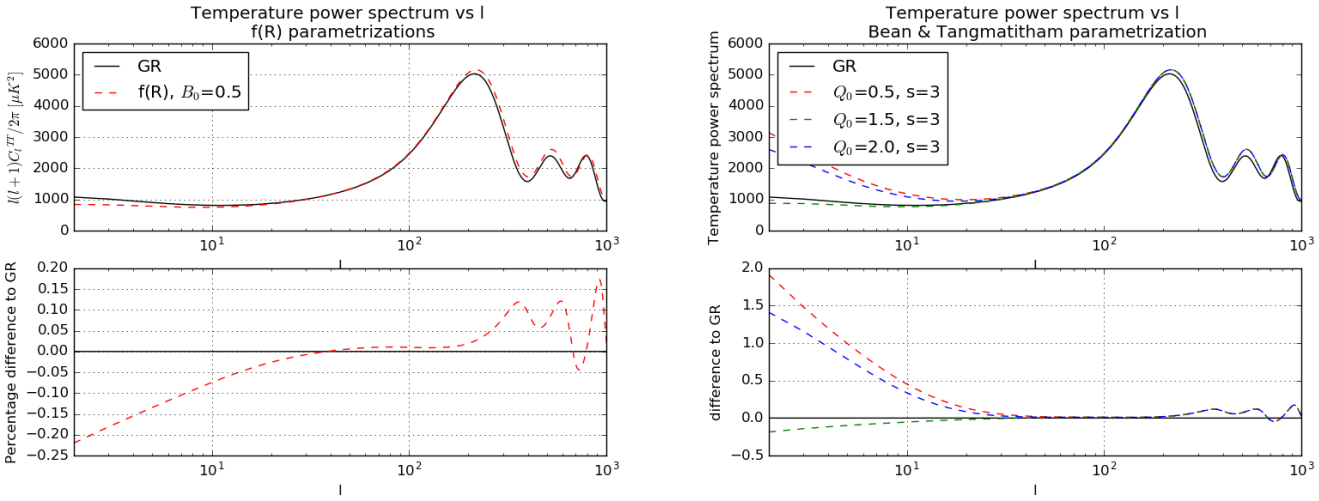

Figure 2: Effect of MG on Temperature power spectrum, according to $f(R)$ theories (top left) and BT parametrization with Q and R evolve (top right) for different values of Q_0. In each case, the difference between MG and GR predictions are plotted underneath. The predictions differ most significantly at low multipoles, corresponding to large angular scales.

Planck is an all-sky survey conducted by the European Space Agency, which measures anisotropies in temperature and polarization of the cosmic microwave background radiation (CMB) with unprecedentedly high accuracy and level of detail [10]. We used data from Planck to constrain the MG parameters.

3.2 Weak lensing surveys

Weak lensing is the effect whereby light is bent when passing through a massive object along the line of sight, causing distortion in the images of the objects behind that mass. This effect is very weak. It requires objects as massive as a galaxy cluster for the effect to become noticeable.

Distortion of the shapes of distant galaxies by large-scale structures is dependent on the two scalar metric potentials, Φ and Ψ, which are as defined in Section 2. This dependency

arises in the formulation of the galaxy lensing convergence spectrum [18]

$$P_{ij}^{k}(l) \approx 2\pi^2 l \int \frac{\mathrm{d}\chi}{\chi} g_i(\chi) g_j(\chi) P_{\Phi+\Psi}(l/\chi, \chi) \tag{20}$$

where χ is the comoving distance, $P_{\Phi+\Psi}$ is the Weyl potential, $g_i(\chi)$ is the lensing efficiency and is defined as

$$g_i(\chi) = \int_{\chi}^{\infty} \mathrm{d}\chi' n_i(\chi') \frac{\chi' - \chi}{\chi'} \tag{21}$$

It is useful to illustrate the effect of MG on the correlation functions $\xi_{i,j}^{\pm}(\theta)$ which have a dependency on the galaxy lensing convergence spectrum [18] and hence on MG

$$\xi_{i,j}^{\pm}(\theta) = \frac{1}{2\pi} \int \mathrm{d}l \, l P_{i,j}^{k}(l) J_{\pm}(l\theta) \tag{22}$$

where J_+ and J_- correspond to the J_0 and J_4 Bessel functions respectively. The effect is demonstrated in figure 3 [13, 14, 15, 16, 17, 7, 19, 20, 21]. The two correlation functions, $\xi_+(\theta)$ and $\xi_-(\theta)$, are plotted against the angular scale, θ(arcmin) for different MG models and for GR. The shifts from GR due to MG for both functions are noticeable over a wide range of angular scales but become less substantial at small scales.

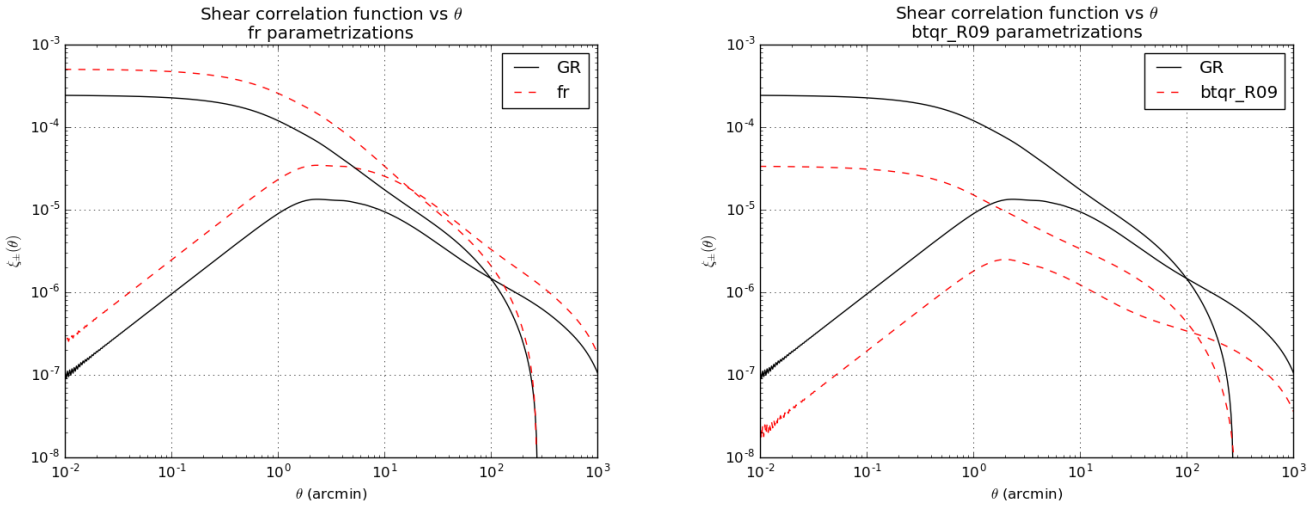

Figure 3: Effect of MG on shear correlation functions, $\xi_+(\theta)$ (upper curve) and $\xi_-(\theta)$ (lower curve), with MG model being: f(R) theories with $B_0 = 0.5$ (left) and BT parametrization with Q, R fixed, $Q = 1.0, R = 0.9$ (right). This is shown for the low-high redshift regions for each MG model. The shifts from GR due to MG for both functions are noticeable over a wide range of angular scales but become less significant at small scales.

We used lensing data from the Canada-France-Hawaii Telescope Survey, which is currently the largest weak-lensing survey, to constrain our MG models.

4 Methodology

We used CosmoSIS, a code developed by J. Zuntz *et al.*, to process the data and provide constraints for the parameters of MG models. The main goal of CosmoSIS is to connect together existing codes for cosmological parameter estimation. Details and tutorials for CosmoSIS can be found in [3] and [22]. The code has several sampling methods implemented in it which the user can easily switch between. Data sets and likelihood functions can be combined for better constraints as long as the user is aware of possible dependency between them. In this project, we used the following three sampling methods: the Metropolis-Hastings algorithm (implemented in CosmoSIS as 'metropolis') [23], the Affine Invariant Markov chain Monte Carlo Ensemble sampler ('emcee') [24] and the Nested sampling algorithm ('multinest') [25, 26, 27]; the advantages and disadvantages when using each of them to constrain MG parameters are explored in section 5. We refer to them by their name in CosmoSIS for brevity.

4.1 Sampling methods and modules

In this section, we describe the algorithms of the three sampling methods that were used.

First, metropolis calculates the likelihood of a point in the sampling space given the data inputted, which is defined by the user or chosen at random. It then randomly chooses another point nearby and calculates the likelihood of this point; if it is greater than the likelihood of the previous point, the new point will be accepted and the next iteration will start from it, otherwise, it will be rejected and the sampler starts over again from the old point. This process repeats until it reaches the required number of samples, which was defined by the user at the beginning. Thus, the sampler will tend to stay in region of high likelihood and occasionally visit low-likelihood points. This information is then displayed on a contour plot, with the darker contours represent regions of higher likelihood in the parameter space. Emcee works on the same principle except that it has many 'walkers' exploring the sampling space simultaneously, and therefore is highly parallelizable and can be considerably faster than metropolis. On the other hand, multinest starts with more than one point (typically a few hundred for cosmological problems), whose likelihoods are then computed and saved, and the ones with least likelihoods will be updated with new points of higher likelihoods using some Markov Chain Monte Carlo steps.

We used the MGCAMB module in CosmoSIS (the Modified Gravity Code for Anisotropies in the Microwave Background), a code written by A. Hojjati *et al.* [17, 7] to evolve the perturbations in the early Universe into the CMB and matter power spectra according to various MG models. Other modules are also included for smoothness of the programme and to convert the outputs from MGCamb into useful statistics for further study. First, we ran the code once using only the anisotropy measurements from Planck, then again with the weak lensing data from CFHTLenS in addition in order to compare the difference.

4.2 Methodology and priors

The samplers we used, especially metropolis, are sensitive to the starting point. The closer this point is to the point of maximum likelihood, the faster it is for the samples to converge. Therefore, we ran the code once using 'maxlike', a sampler which aims at finding the points of maximum likelihood of the parameters, then used the outputs from maxlike as priors for the metropolis, emcee or multinest sampler. Note that maxlike sampled over the cosmological parameters only whose starting points were the values found from Planck data as proposed in [1], while the MG parameters were kept fixed at their GR values. This is to make sure the code does not behave strangely. In the next run with the metropolis/emcee/multinest sampler, we sampled over both cosmological parameters and MG parameters, with the starting points being those of maximum likelihood as found with the maxlike sampler for cosmological parameters, and the GR values for MG parameters. The cosmological parameters we sampled were the matter density parameter (Ω_m), baryon density parameter (Ω_b), reduced Hubble's constant ($h_0 = H_0/100$ with H_0 being the Hubble's constant), reionization optical depth (τ), scalar spectral index (n_s) and the curvature power spectrum at $k_0 = 0.05\text{Mpc}^{-1}$ (A_s). Tables 1 [1] and 2 presents the priors used by maxlike and by metropolis/emcee/multinest samplers.

Cosmological Parameter	Planck value	Sampling range
Ω_m	0.3	[0.2, 0.4]
h_0	0.68	[0.6, 0.8]
Ω_b	0.04	[0.02, 0.06]
τ	0.08	none
n_s	0.96	[0.94, 0.98]
A_s	2.1e-9	[1.9e-9, 2.3e-9]

Table 1: Priors for Cosmological parameters (used by maxlike sampler)

MG Parameter	GR value	Sampling range	MG model
B_0	0.0	[0.0, 6.0]	$f(R)$
Q	1.0	[0.0, 10.0]	Bean-Tangmatitham
R	1.0	[-1.0, 10.0]	Q, R fixed
Q_0	1.0	[0.0, 10,0]	Bean-Tangmatitham
R_0	1.0	[-1.0, 10,0]	Q, R evolve
s	0.0	[0.0, 3.0]	

Table 2: Priors for MG parameters (used by metropolis/emcee/multinest sampler)

5 Results

First, we ran CosmoSIS using all three sampling methods (metropolis, emcee and multinest) to estimate the cosmological parameters when no MG is present. Our purpose was to test the code and to determine which sampler would be the best for constraining MG parameters. Of all three samplers, metropolis was the slowest (it showed no sign of convergence even

after 80,000 samples) and emcee was the fastest (converged after running through 25,000 samples). Multinest was not too far behind: it converged after 29,000 samples. As both emcee and multinest are parallelizable, they are much faster than metropolis. Multinest gives the most objective estimations of all three samplers as it explores the whole sample space, whereas metropolis and emcee are localised around a point of maximum likelihood and thus their estimations may vary noticeably with the starting point. However, we have good reasons to believe that the MG parameters should not be too far away from their GR values as GR has survived many high precision tests, therefore, the estimations from multinest and metropolis/emcee should be similar, as long as the starting point is set to the GR values. All in all, we chose emcee over the other two for its speed.

5.1 Constraints on f(R) parameters

Data / Parameter	Planck (40,000 samples)	Planck+CFHTLenS (10,000 samples)	
Ω_m	0.356 ($\pm$0.025)	0.26 ($\pm$0.04)	Cosmological parameters
h_0	0.639 ($\pm$0.016)	0.71 ($\pm$0.04)	
Ω_b	0.0498 ($\pm$0.0019)	0.043 ($\pm$0.007)	
n_s	0.942 ($\pm$0.010)	0.9686 ($\pm$0.0015)	
A_s	2.21543 ($\pm$0.021) $\times 10^{-09}$	2.14 ($\pm$0.11) $\times 10^{-09}$	
B_0	0.67 ($\pm$1.11)	0.03 ($\pm$2.97)	MG parameters

Table 3: Contraints on cosmological and MG parameters at 95% confidence level for $f(R)$ theories using different data sets.

Table 3 presents the constraints on cosmological parameters and B_0, the parameter of $f(R)$ theories [13, 14, 15, 16, 17, 7, 19, 20, 21]. In the first column, except for Ω_b and A_s, all the other cosmological parameters are not consistent with the values obtained by the Planck collaboration [1] though they are quite close. One possible reason is because we did not include the lensing effect in the theoretical power spectrum computed by the code. On the other hand, the cosmological parameters estimated when using CFHTLenS in addition to Planck data are consistent with those obtained by the Planck collaboration. The estimation for B_0 from both sets of data are consistent with GR, corresponding to $B_0 = 0.0$, at 95% confidence level. However, we should note that the estimations obtained with Planck+CFHTLenS are not reliable as there was an error which gave rise to nonesensical values of the parameters after 10,000 samples at which point the programme aborted automatically even though none of the parameters had reached convergence. The real cause of it is unknown, but it may be because we used all the data sets from CFHTLenS surveys, which are not neccesarily independent of one another. As the constraints obtained with Planck+CFHTLenS data are poor (especially for B_0), we will only present the results from Planck data for other MG models.

The results we obtained are encoded in figures 4 and 5. Figure 4 shows 95% and 68% contour plots produced by 40,000 samples, with the first 10,000 being ignored as they may contain more statistical noise than the rest [13, 14, 15, 16, 17, 7]. B_0 shows no correlation with the cosmological parameters. The latter has better (tighter) constraints. The constraints given

by 10,000 samples using Planck+CFHTLenS data are poor, as shown in figure 5 [13, 14, 15, 16, 17, 7, 19, 20, 21]. More samples will need to be collected if we could fix the error in the programme.

5.2 Constraints on BT parameters

5.2.1 Q(a,k) and R(a,k) fixed

Parameter \ Data	Planck (10,000 samples)	
Ω_m	0.340 ($\pm$0.019)	Cosmological parameters
h_0	0.651 ($\pm$0.014)	
Ω_b	0.0483 ($\pm$0.0018)	
n_s	0.941 ($\pm$0.008)	
A_s	2.27 ($\pm$0.09) $\times 10^{-09}$	
Q	1.04 ($\pm$0.06)	MG parameters
R	0.97 ($\pm$0.05)	

Table 4: Contraints on cosmological and MG parameters at 95% confidence level for BT parametrization with $Q(a,k)$ and $R(a,k)$ being constant.

We kept s fixed at the value 3.0 and sampled Q and R only for a first simple approach. An error occured which limited the sampling process to 10,000 samples, the true cause is unknown. The estimations presented in table 4 [13, 14, 15, 16, 17, 7], except for Ω_b and A_s, are inconsistent with those found by the Planck collaboration [1]. The GR value of the parameters are within the 95% confidence level of their estimations.

Figure 6 and 7 present the 2D contour plots of Q and R with the cosmological parameters from 10,000 samples [13, 14, 15, 16, 17, 7]. A linear correlation exists between Q and A_s, while R shows an anti-correlation with A_s and Q, as the plots suggest. The 68% constraints are poor. More samples need to be collected for better constraints. The marginal probability density distributions of Q and R sharply peak near the value 1.0, which is their GR value. This justifies for our statement at the beginning of Section 5.

5.2.2 Q(a,k) and R(a,k) evolving

For this model, we also allowed for s to be sampled. Except for Ω_b and A_s, all the comological paramter estimations are inconsistent with Planck's results [1], as shown in table 5 [13, 14, 15, 16, 17, 7]. One possible reason is as proposed in Section 5.1. The constraints on the MG parameters are consistent with their GR values at 95% confidence level.

Figures 8, 9, 10 and 11 encode the results we obtained [13, 14, 15, 16, 17, 7]. The sampling process was limited to 12,800 samples for some unknown errors. It may be useful to test if this error also arises for other samplers. The constraints are good for all parameters except

Parameter \ Data	Planck (12,800 samples)	
Ω_m	0.357 ($\pm$0.026)	Cosmological parameters
h_0	0.638 ($\pm$0.016)	
Ω_b	0.0499 ($\pm$0.0020)	
n_s	0.9434 ($\pm$0.0075)	
A_s	2.21 ($\pm$0.020) $\times 10^{-09}$	
Q_0	0.94 ($\pm$0.64)	MG parameters
R_0	1.42 ($\pm$0.93)	
s	2.16 ($\pm$0.77)	

Table 5: Contraints on cosmological and MG parameters at 95% confidence level for BT parametrization with $Q(a,k)$ and $R(a,k)$ evolving.

for n_s and s. More samples are needed for all parameters to converge. The constraints suggest a non-linear correlation between Q_0 and R_0.

6 Conclusion

We used the Affine Invariant Markov chain Monte Carlo algorithm (emcee) together with the data from CMB anisotropy measurements and weak lensing surveys to provide constraints for the cosmological parameters and the parameters of our MG models. The constraints on cosmological parameters are close but not consistent with those stated by Planck collaboration [1]. This may be because we did not include lensing effects in our theoretical calculations which caused a shift in the estimations. Constraints on the parameters of all MG models indicate GR is still a likely possibility as their GR values lie within 95% confidence level of the estimations. The programme faced some unknown error that limited the number of samples being recorded and made the constraints less reliable in some cases. This is possibly because we included all the data sets from the CFHTLenS surveys, which are not neccessarily independent and made the samples to move off to extreme values quickly. Collecting more samples may make the process to eventually move away from the region of extreme values and increase the number of samples being recorded, thus leads to better constraints. It might also be useful to see if this error arises for samplers other than emcee, then we may have a better diagnosis for the problem.

Because of the time limit, we did not have time to produce the estimations with other algorithms. It might be interesting to do so and compare their results.

All in all, we have found no deviation from GR for the MG parameters at 95% confidence level. More sensitive measurements in the future may yield a different result, but for the time being, there is not enough evidence to reject GR. MG remains an open possibility. We should also consult other mechanisms to explain the accelerated expansion of the universe.

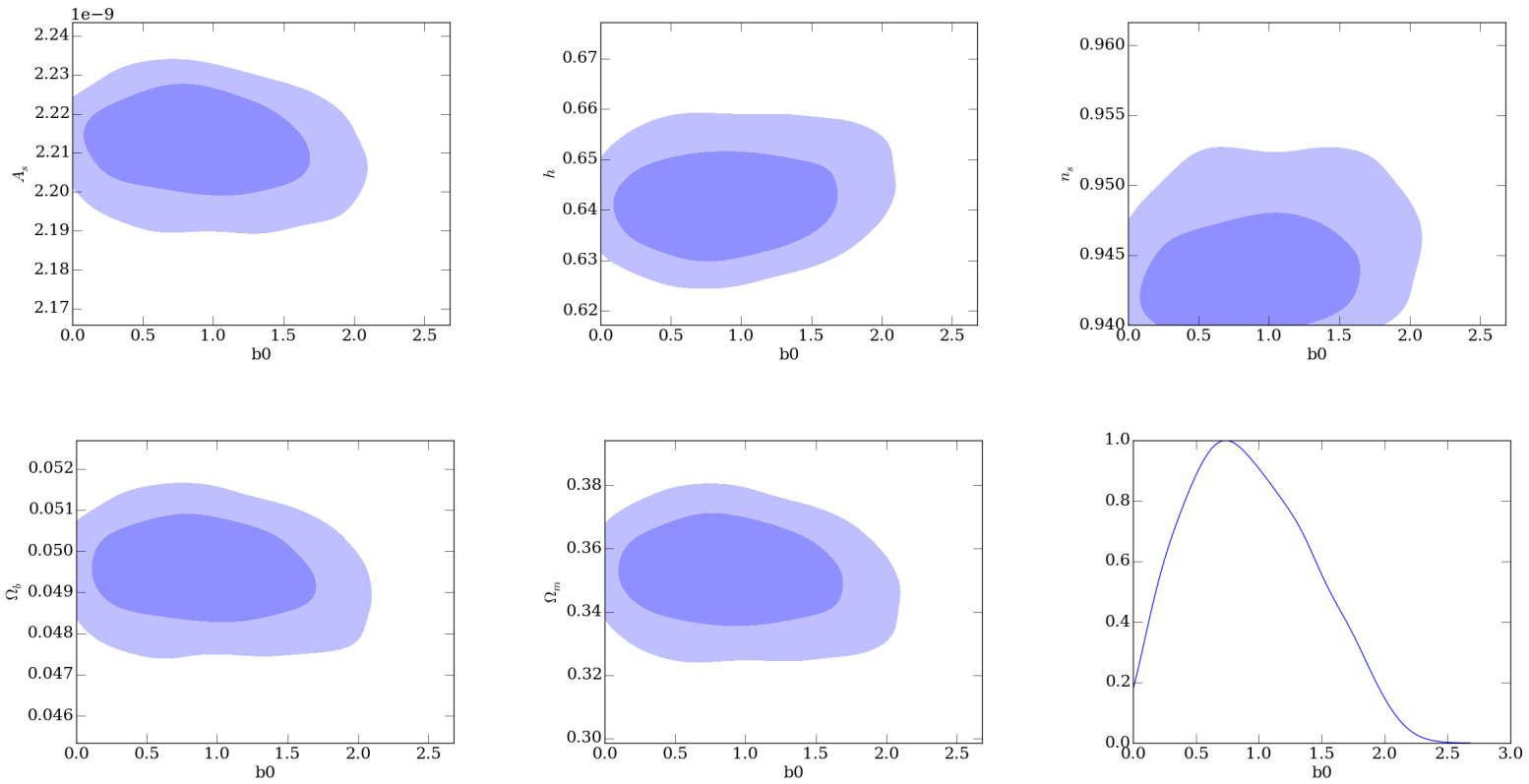

Figure 4: 95% and 68% confidence level contours for B_0 with other cosmological parameters, and marginal probability density distribution of B_0 (bottom right), using Planck data. These are constraints from 40,000 samples. We ignored the first 10,000 samples as they may contain more statistical noise than the rest. The 2D contours indicate B_0 are not correlated to other cosmological parameters. The constraints are tighter for the latter.

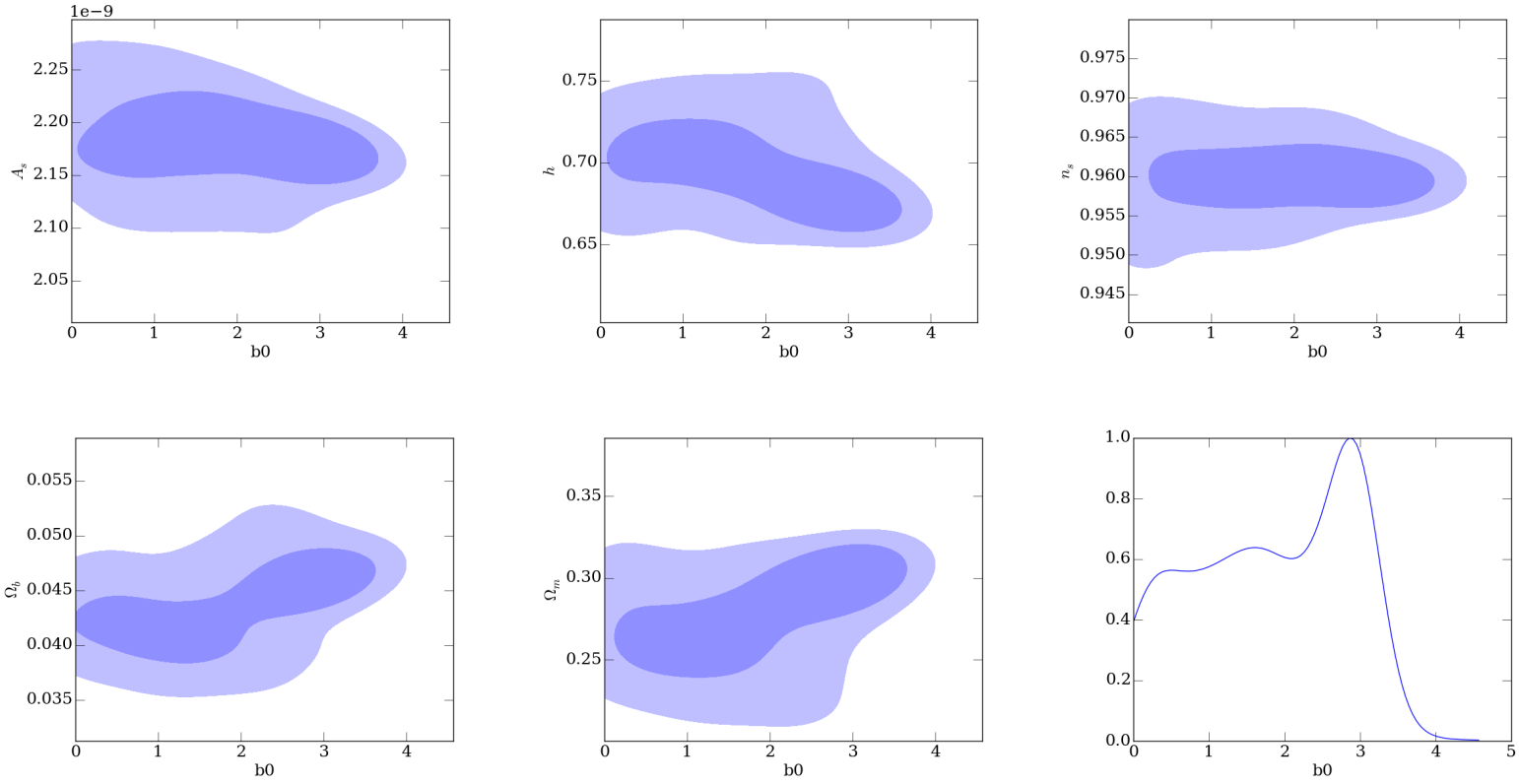

Figure 5: 95% and 68% confidence level contours for B_0 with other cosmological parameters, and marginal probability density distribution of B_0 (bottom right), using Planck+CFHTLenS data. The constraints are poor for 10,000 samples.

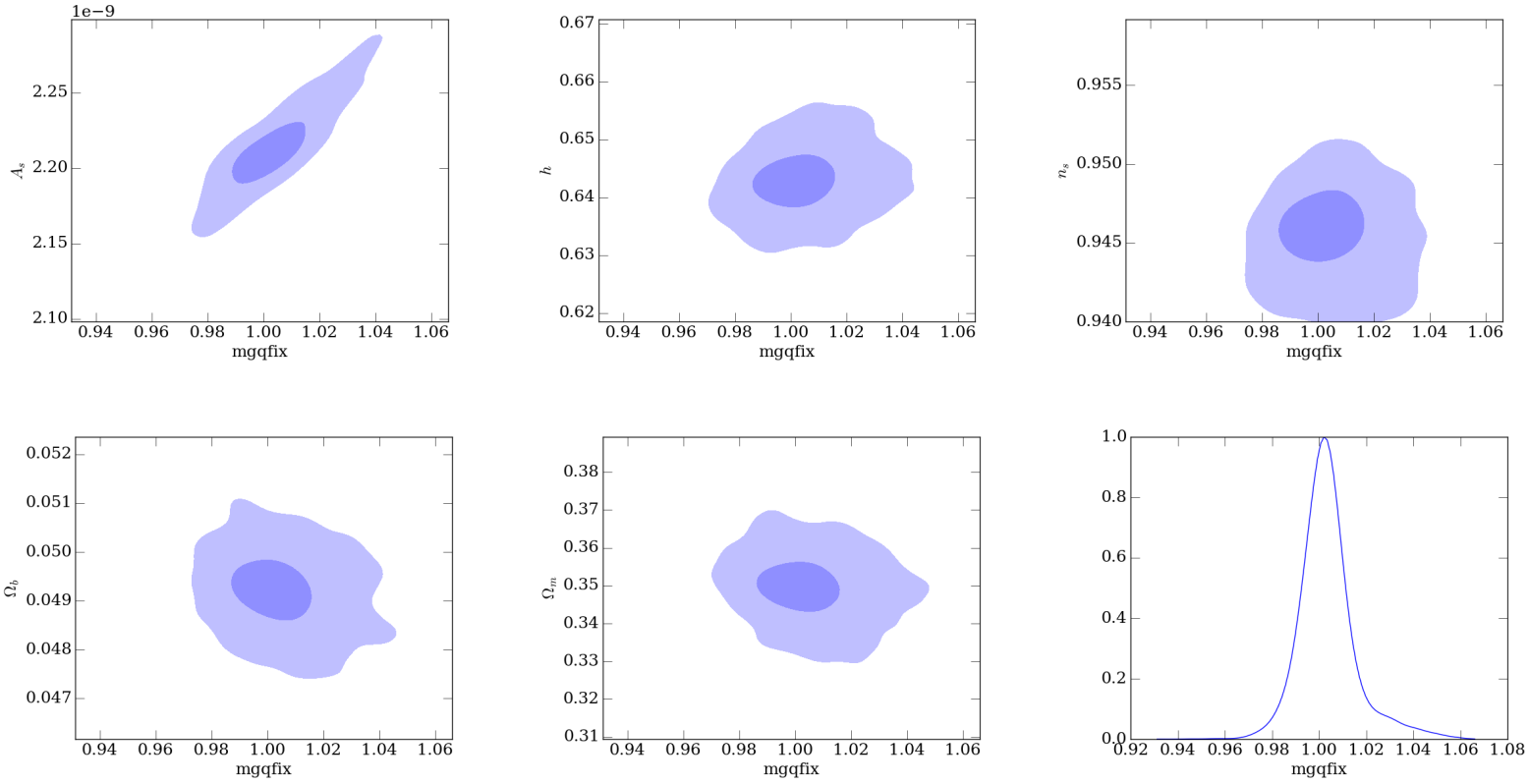

Figure 6: 95% and 68% confidence level contours for Q with other cosmological parameters, and marginal probability density distribution of Q (bottom right), using Planck data. The process was limited to 10,000 samples for some unknown reason. Q and A_s are correlated.

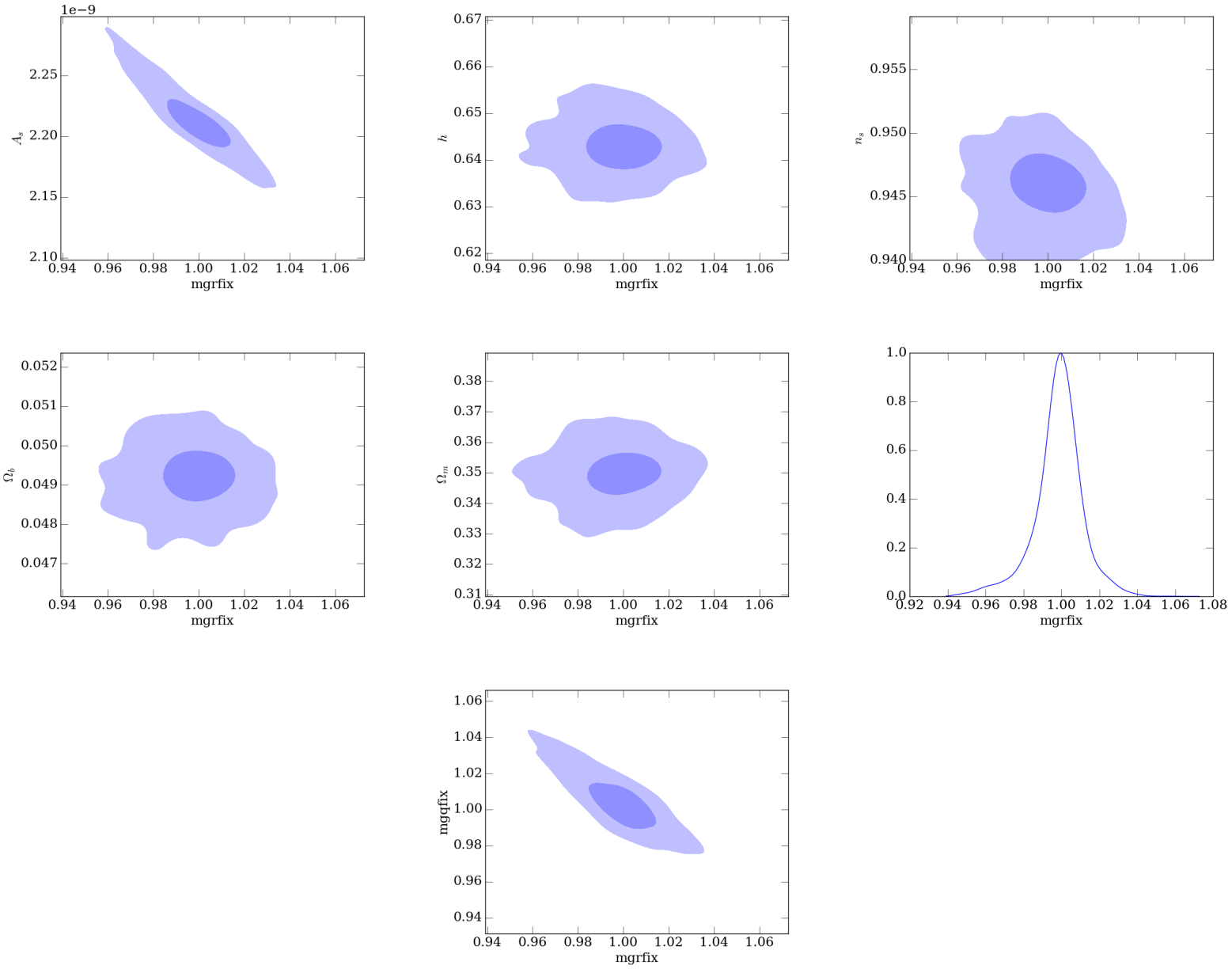

Figure 7: 95% and 68% confidence level contours for R with other cosmological parameters, and marginal probability density distribution of R (middle right), using Planck data. The 68% constraints are poor. R and A_s have a linear anti-correlation and so do R and Q.

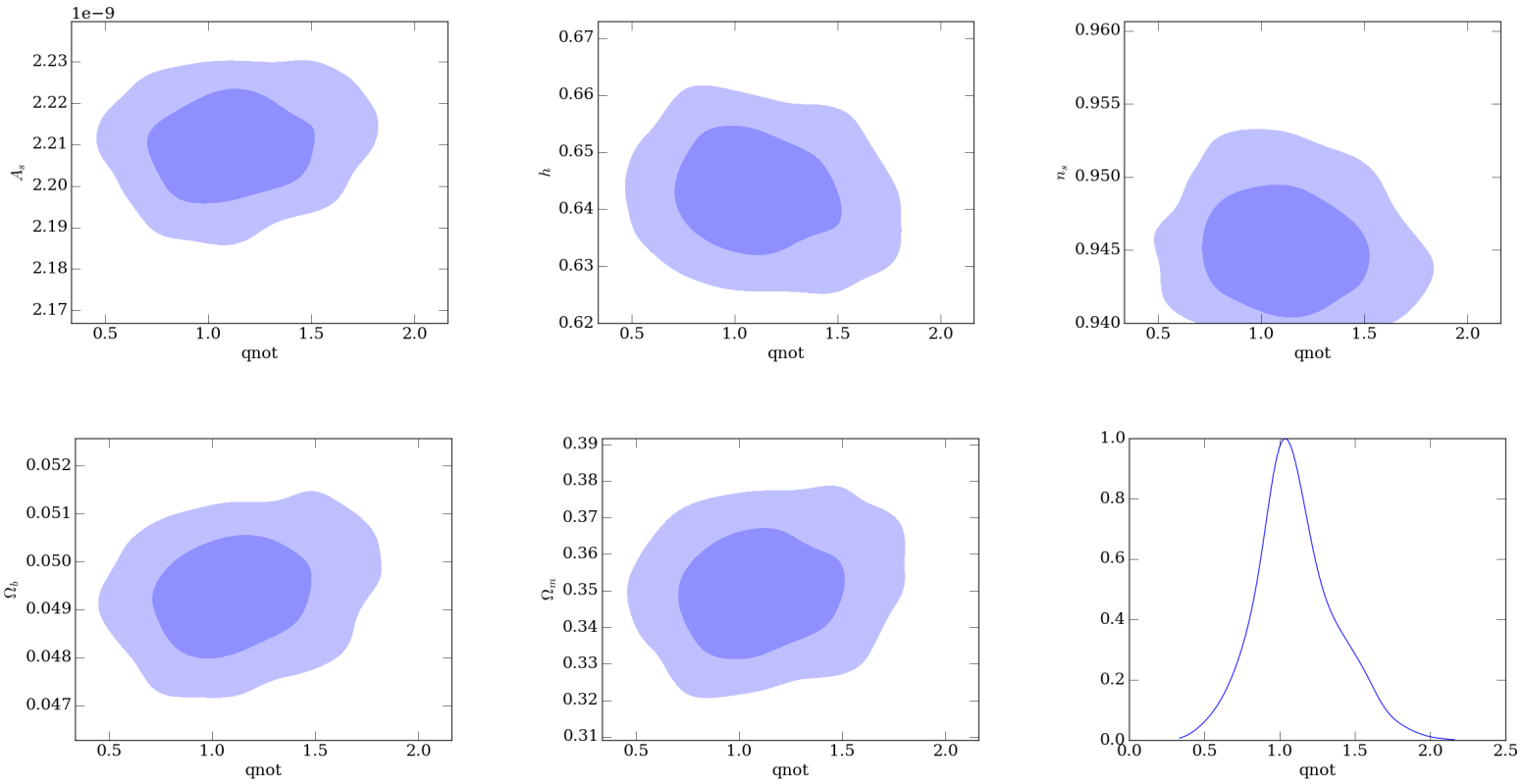

Figure 8: 95% and 68% confidence level contours for Q_0 with other cosmological parameters, and marginal probability density distribution of Q_0 (bottom right), using Planck data. The process was limited to 12,800 samples at which point the programme aborted automatically. One possible reason is the walkers move towards extreme values towards the end and make the sampler (emcee) behave badly. The constraints are good for all paramters except for n_s. More samples are needed for all the parameters to converge. Q_0 and the cosmological parameters are not correlated.

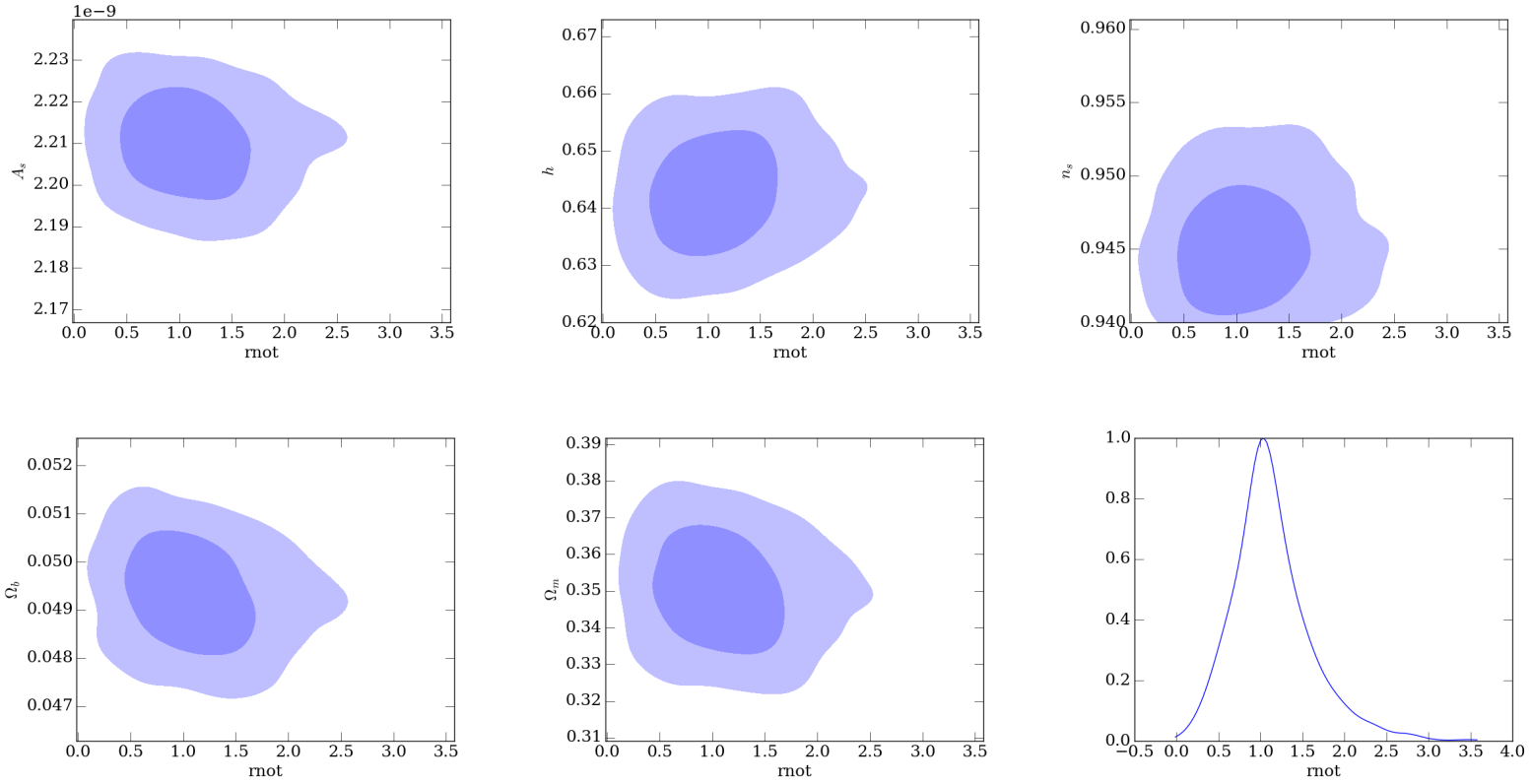

Figure 9: 95% and 68% confidence level contours for R_0 with other cosmological parameters, and marginal probability density distribution of R_0 (bottom right), using Planck data. R_0 and the cosmological parameters are not correlated.

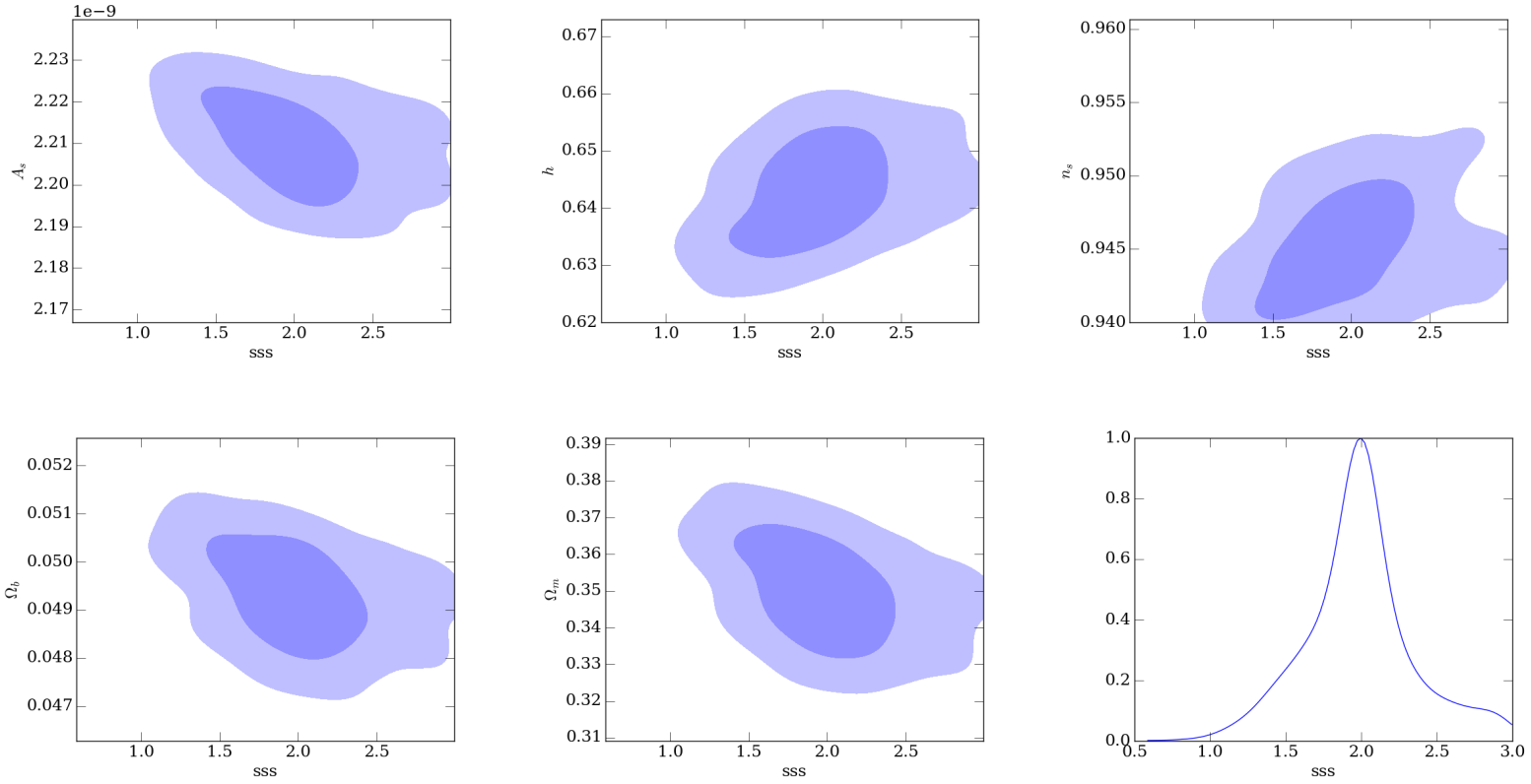

Figure 10: 95% and 68% confidence level contours for s with other cosmological parameters, and marginal probability density distribution of s (bottom right), using Planck data. The constraints are poor but they suggest that s is correlated to h_0 and n_s and is anti-correlated to A_s, Ω_b and Ω_m.

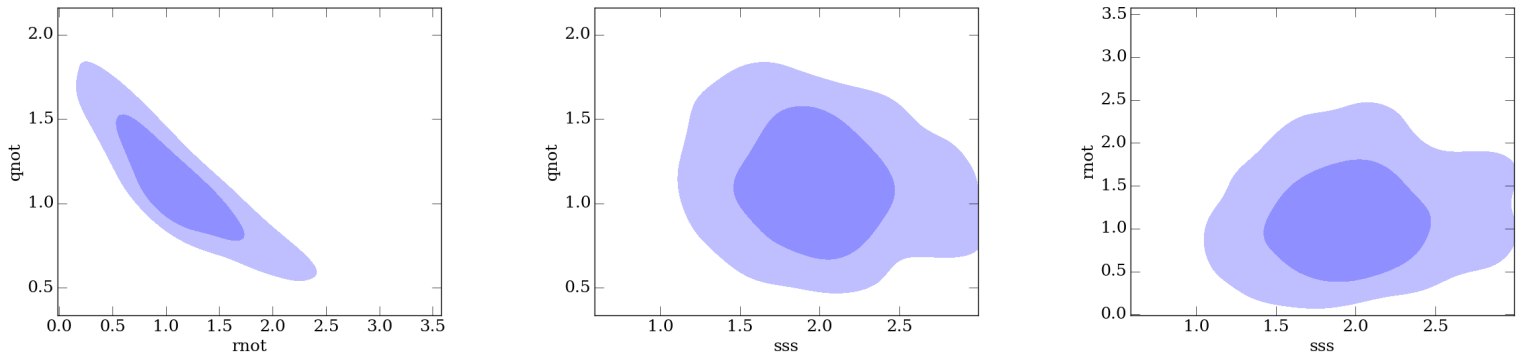

Figure 11: 95% and 68% confidence level contours of BT parameters with one another, using Planck data. The constraints suggest a non-linear correlation between Q_0 and R_0.

References

[1] P. A. R. Ade *et al.*, "Planck 2015 results. XIII. Cosmological parameters," 2015, 1502.01589.

[2] A. G. Riess *et al.*, "Observational evidence from supernovae for an accelerating universe and a cosmological constant," *Astron. J.*, vol. 116, pp. 1009–1038, 1998, astro-ph/9805201.

[3] J. Zuntz, M. Paterno, E. Jennings, D. Rudd, A. Manzotti, S. Dodelson, S. Bridle, S. Sehrish, and J. Kowalkowski, "CosmoSIS: Modular Cosmological Parameter Estimation," *Astron. Comput.*, vol. 12, pp. 45–59, 2015, 1409.3409.

[4] R. Bean and M. Tangmatitham, "Current constraints on the cosmic growth history," *Phys. Rev. D*, vol. 81, p. 083534, Apr. 2010, 1002.4197.

[5] A. De Felice and S. Tsujikawa, "f(R) theories," *Living Rev. Rel.*, vol. 13, p. 3, 2010, 1002.4928.

[6] T. Giannantonio, M. Martinelli, A. Silvestri, and A. Melchiorri, "New constraints on parametrised modified gravity from correlations of the CMB with large scale structure," *J. Cosmol. Astropart. Phys.*, vol. 4, p. 030, Apr. 2010, 0909.2045.

[7] G.-B. Zhao, L. Pogosian, A. Silvestri, and J. Zylberberg, "Searching for modified growth patterns with tomographic surveys," *Phys. Rev. D*, vol. 79, p. 083513, 2009, 0809.3791.

[8] G. Magnano and L. M. Sokolowski, "On physical equivalence between nonlinear gravity theories and a general relativistic selfgravitating scalar field," *Phys. Rev. D*, vol. 50, pp. 5039–5059, 1994, gr-qc/9312008.

[9] C.-P. Ma and E. Bertschinger, "Cosmological perturbation theory in the synchronous and conformal Newtonian gauges," *Astrophys. J.*, vol. 455, pp. 7–25, 1995, astro-ph/9506072.

[10] J. Tauber, M. Bersanelli, J. M. Lamarre, G. Efstathiou, C. Lawrence, F. Bouchet, E. Martinez-Gonzalez, S. Matarrese, D. Scott, M. White, *et al.*, "The Scientific programme of Planck," 2006, astro-ph/0604069.

[11] C. Heymans *et al.*, "CFHTLenS tomographic weak lensing cosmological parameter constraints: Mitigating the impact of intrinsic galaxy alignments," *Mon. Not. Roy. Astron. Soc.*, vol. 432, p. 2433, 2013, 1303.1808.

[12] R. K. Sachs and A. M. Wolfe, "Perturbations of a cosmological model and angular variations of the microwave background," *Astrophys. J.*, vol. 147, pp. 73–90, 1967. [Gen. Rel. Grav.39,1929(2007)].

[13] Z. Hou *et al.*, "Constraints on Cosmology from the Cosmic Microwave Background Power Spectrum of the 2500 deg^2 SPT-SZ Survey," *Astrophysical Journal*, vol. 782, p. 74, feb 2014, 1212.6267.

[14] P. A. R. Ade *et al.*, "Planck 2013 results. XV. CMB power spectra and likelihood," *Astron. Astrophys.*, vol. 571, p. A15, 2014, 1303.5075.

[15] J. Dunkley *et al.*, "The Atacama Cosmology Telescope: likelihood for small-scale CMB data," *J. Cosmol. Astropart. Phys.*, vol. 1307, p. 025, 2013, 1301.0776.

[16] G. Hinshaw *et al.*, "Nine-year Wilkinson Microwave Anisotropy Probe (WMAP) Observations: Cosmological Parameter Results," *Astrophysical Journal Supplement*, vol. 208, p. 19, Oct. 2013, 1212.5226.

[17] A. Hojjati, L. Pogosian, and G.-B. Zhao, "Testing gravity with CAMB and CosmoMC," *J. Cosmol. Astropart. Phys.*, vol. 1108, p. 005, 2011, 1106.4543.

[18] P. A. R. Ade *et al.*, "Planck 2015 results. XIV. Dark energy and modified gravity," 2015, 1502.01590.

[19] R. Takahashi, M. Sato, T. Nishimichi, A. Taruya, and M. Oguri, "Revising the Halofit Model for the Nonlinear Matter Power Spectrum," *Astrophys. J.*, vol. 761, p. 152, 2012, 1208.2701.

[20] R. E. Smith, J. A. Peacock, A. Jenkins, S. D. M. White, C. S. Frenk, F. R. Pearce, P. A. Thomas, G. Efstathiou, and H. M. P. Couchmann, "Stable clustering, the halo model and nonlinear cosmological power spectra," *Mon. Not. Roy. Astron. Soc.*, vol. 341, p. 1311, 2003, astro-ph/0207664.

[21] M. Kilbinger *et al.*, "Dark energy constraints and correlations with systematics from CFHTLS weak lensing, SNLS supernovae Ia and WMAP5," *Astron. Astrophys.*, vol. 497, p. 677, 2009, 0810.5129.

[22] "CosmoSIS wiki page." `https://bitbucket.org/joezuntz/cosmosis/wiki/Home`. Retrieved: 2016-09-14.

[23] W. K. Hastings, "Monte Carlo sampling methods using Markov chains and their applications," *j-BIOMETRIKA*, vol. 57, pp. 97–109, Apr. 1970.

[24] J. Goodman and J. Weare, "Ensemble Samplers with Affine Invariance," *Commun. Appl. Math. Comput. Sci.*, vol. 5, pp. 65–80, 2010.

[25] F. Feroz, M. P. Hobson, and M. Bridges, "MultiNest: an efficient and robust Bayesian inference tool for cosmology and particle physics," *Mon. Not. Roy. Astron. Soc.*, vol. 398, pp. 1601–1614, 2009, 0809.3437.

[26] F. Feroz and M. P. Hobson, "Multimodal nested sampling: an efficient and robust alternative to MCMC methods for astronomical data analysis," *Mon. Not. Roy. Astron. Soc.*, vol. 384, p. 449, 2008, 0704.3704.

[27] F. Feroz, M. P. Hobson, E. Cameron, and A. Pettitt, "Importance Nested Sampling and the MultiNest Algorithm," 2014, 1306.2144.